Investigation of Mechanical & Thermal Properties of Pulsed Current Micro Plasma Arc Welded Aluminum (Al-6061) Alloy

¹Venkata Sai, ²N. Pallavi Senapati

¹M. Tech Student, Department of Mechanical Engineering, Nadimpalli Satyanarayana Raju Institute of Technology, Visakhapatnam, AP, INDIA

Abstract: - In the present work pulsed current Micro Plasma Arc Welding (MPAW) process is used to join 0.5mm thick sheets of Aluminium (Al-6061) alloy by selecting proper welding parameters namely peak current, base current, pulse rate and pulse width are the most influencing parameters affecting the quality of the weld joint. Trial experiments are carried out using the selected welding parameters to fix the number of levels of each welding parameter. For four factors and five levels, Taguchi L25 orthogonal design matrix is adopted to find the number of experiments to be performed. The mechanical properties such as grain size, hardness and tensile strength are measured as per ASTM standards. Empirical mathematical model is developed for the above weld quality characteristics using MINITAB 20 statistical software considering significant coefficients. Linear equation is adopted in designing the models. The adequacy of the models is tested by Analysis of Variance (ANOVA) at 95% confidence level. The coefficient of determination for the developed models is found to be 0.92. Confirmation experiments are performed to validate the developed models. Lastly, the temperature distribution in the welding sample has been simulated by using ANSYS software. The thermal profiles in different welding zones have been studied in detail and linked to the mechanical properties of the joint.

Keywords: - Micro Plasma Arc Welding, ANOVA, Tensile strength, grain size

1. Introduction

The plasma arc welding process was introduced to the welding industry in 1964 as a method of bringing better control to the arc welding process in lower current ranges [4]. Today, plasma retains the original advantages it brought to the industry by providing an advanced level of control and accuracy to produce high quality welds in both miniature and pre precision applications and to provide long electrode life for high production requirements at all levels of amperage. Plasma welding is equally suited to manual and automatic applications. It is used in a variety of joining operations ranging from welding of miniature components to seam welding, to high volume production welding, and many others.

The plasma arc technology is industrially used for plasma arc cutting, plasma powder build-up welding, plasma powder joint welding, plasma wire build-up welding, plasma spraying and plasma joint welding. The field of applications is ranged from thin sheets with thicknesses from 0.1 mm to 1.5 mm, which are welded by the micro plasma welding technique, to the plasma needle hole welding for thicknesses from 2.5mm to 10mm to weld in butt joint. The plasma arc welding can be regarded as a further development of the tungsten inert gas (TIG)-

²Assistant Professor, Department of Mechanical Engineering, Nadimpalli Satyanarayana Raju Institute of Technology, Visakhapatnam, AP, INDIA



Volume: 09 Issue: 07 | July - 2025 SJIF Rating: 8.586 **ISSN: 2582-3930**

technique.

1.1 Working Principle of Plasma Arc Welding

Plasma is a gas which is heated to an extremely high temperature and ionized so that it becomes electrically conductive. Similar to GTAW (TIG), the PAW process uses this plasma to transfer an electric arc to a workpiece [4]. The metal to be welded is melted by the intense heat of the arc and fuses together. A comparison of TIG/GTAW and Plasma welding arcs are shown in Fig.1.1.

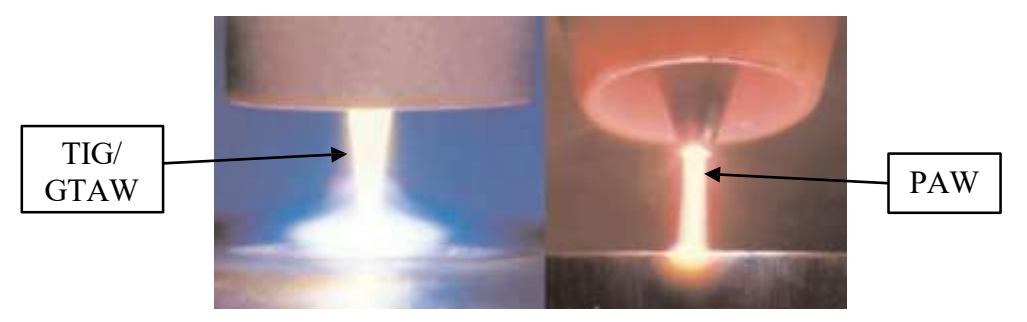
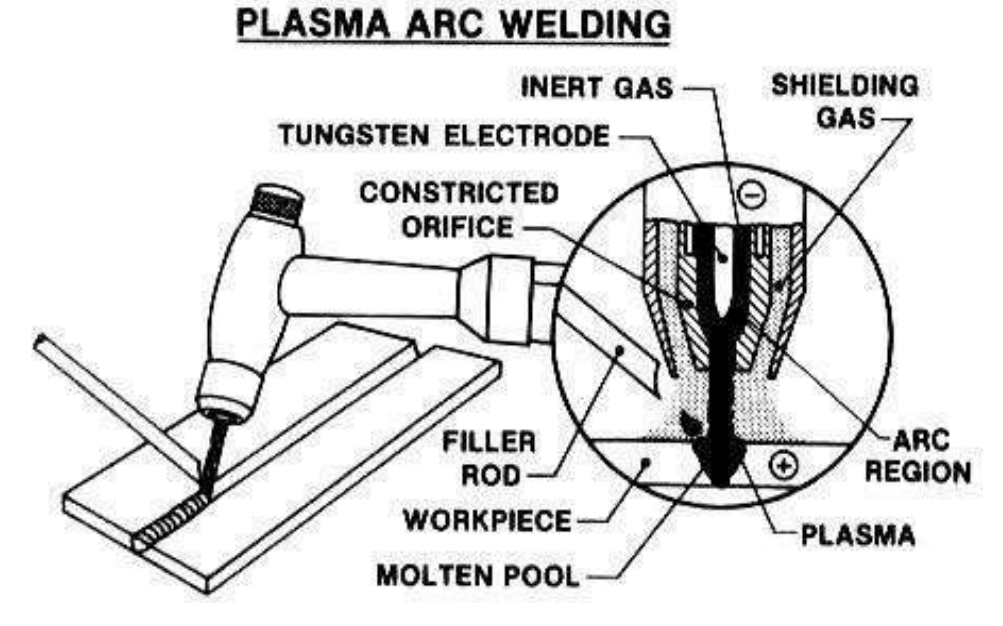


Fig. 1.1: A comparison of the TIG/GTAW (left) and Plasma (right) welding arcs [4]

In the plasma welding torch a Tungsten electrode is located within a copper nozzle having a small opening at the tip. A pilot arc is initiated between the torch electrode and nozzle tip. This arc is then transferred to the metal to be welded. By forcing the plasma gas and arc through a constricted orifice, the torch delivers a high concentration of heat to a small area. With high performance welding equipment, the plasma process produces exceptionally high quality welds. Plasma gases are normally argon. The torch also uses a secondary gas which can be argon, argon /hydrogen, or helium, which assists in shielding the molten weld puddle thus minimizing oxidation of the weld. In order to perform plasma arc welding, the following is required: a power supply; a plasma console (sometimes external, sometimes built in); a water recirculatory (sometimes external, sometimes built in); a plasma welding torch; and a torch accessory kit (tips, ceramics, collets, electrodes, and setup gages). Details about Plasma Arc Welding are shown in Fig.1.2



.Fig. 1.2: Plasma arc welding

Luca Boccarusso et al. [22] analyzed that Ti-6Al-4V is an alloy increasingly used in aeronautics due to its high mechanical properties coupled with lightness. Ti- 6Al-4V rolled sheets 3.2 mm thick were welded in butt joint configuration using a laser source and their performance was studied in terms of weld morphology, microstructure, Vickers micro hardness and fatigue life. Anil Patnaik et al. [23] fabricated the beams from welding plates and the maximum and minimum load values at which the built-up beams were cyclically deformed were chosen to be within the range of 22-45% of the maximum predicted flexural static load. Hong-Yu Qi et al. [24] studied about Electron beam welding (EBW) has been widely used in the manufacture of aluminium alloy welded blisk for aircraft engines. The results show that fatigue crack growth rate increases as the experimental load increases under the same stress ratio and stress intensity factor range. T.S. Balasubramanian et al. [25] analyzed the fatigue crack growth behavior of gas tungsten arc, electron beam and laser beam welded Al6061 alloy. A 100kN servo hydraulic controlled fatigue testing machine was used under constant amplitude uniaxial tensile load (stress ratio of 0.1 and frequency of 10 Hz). S.Q. Wang et al. [26] investigated the micro structural change and fatigue resistance of electron beam welded (EBWed) dissimilar joints between Ti-6Al-4V and BT9 (Ti-6.5Al-3.5Mo-1.5Zr) alloys after two types of post-weld heat treatment (PWHT), namely only aging and solution treatment followed by aging (STA). Mirco Daniel Chapetti et al. [27] studied about a simple expression is proposed to estimate the fatigue endurance of welded joints that can be used to understand and analyze in a simple way the influence of the main geometrical, mechanical and material effects (weld geometry, local geometry, material properties, residual stresses and size of defects). Hong-Yu Qi et al. [28] carried out low cycle fatigue (LCF) tests using symmetrical cyclic loading under total strain amplitude control conditions. The present paper is devoted to investigating the cyclic deformation response of aluminium and the electron-beam-welded (EBW) joint in the following aspects, i.e., cyclic deformation behavior, fatigue life and fatigue fracture behavior. S.T. Auwal et al. [29] investigated that there is an increased in used of titanium alloys for some parts of mass-produced automobiles and aerospace. Fa Xing Che [30] analyzed a method of design-for-reliability (DFR) for the advanced electronic package under temperature cycling (TC) condition is demonstrated, including material characterization, reliability test, finite element analysis (FEA), and fatigue life model development.

From the literature review, it is understood that most of the works in Plasma arc welding (PAW) and its associated phenomena were towards modeling of plasma arc, temperature and heat transformation and process parameter optimization to get the desired weld quality. Most of the works were on mild steel, stainless steel and duplex steels and very few works were reported on Al-6061 alloy, especially of thin sheets of thickness less than one mm. The present work aims in studying mechanical and fatigue properties of micro plasma arc welded Aluminium (Al6061) alloy. The primary objective of this research work is to study the performance of aluminium alloy Al-6061 under both static and fatigue loading conditions.

2. Materials and Methods

Aluminium (Al-6061) sheets of 5 mm thickness were chosen for welding. First the sheets were cut into 100 mm × 200 mm size using shearing machine. Copper sinks are fixed to the fixture to minimize weld distortion and extreme care has been taken for proper cutting of sheets. Square butt joint was selected as the thickness is very small. Details about weld joint dimensions are shown in Fig. 1.

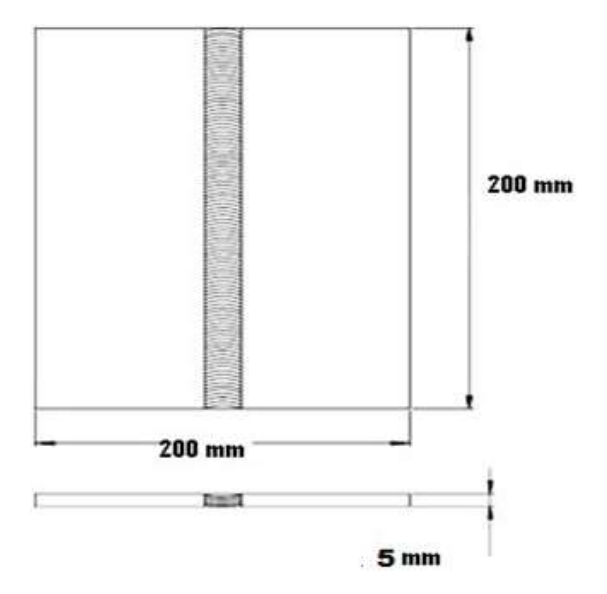


Fig. 1: Dimensions of welded joint

Aluminium (Al-6061) sheets of $100 \times 200 \times 5$ mm are welded autogenously with square butt joint without edge preparation. The chemical composition Aluminium (Al-6061) sheet is given in Table-1. High purity argon gas (99.99%) is used as a shielding gas and a trailing gas right after welding to prevent absorption of oxygen and nitrogen from the atmosphere. The welding has been carried out under the welding conditions. There are many influential process parameters which effect the weld quality characteristics of Pulsed Current MPAW process like peak current, back current, pulse rate, pulse width, flow rate of shielding gas, flow rate of purging gas, flow rate of plasma gas, welding speed etc. From the earlier works [11-13] carried out on Pulsed Current MPAW it was understood that the peak current, back current, pulse rate and pulse width are the dominating parameters which effect the weld quality characteristics. The values of process parameters used in this study are the optimal values obtained from our earlier papers [11-13]. Details about experimental setup are shown in Fig. 2 and fig. 3.

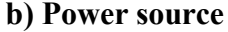
Volume: 09 Issue: 07 | July - 2025

SJIF Rating: 8.586



a) Welding fixture gas cylinders.







ISSN: 2582-3930

c) Plasma and Shielding

Fig. 2: MPAW setup with accessories

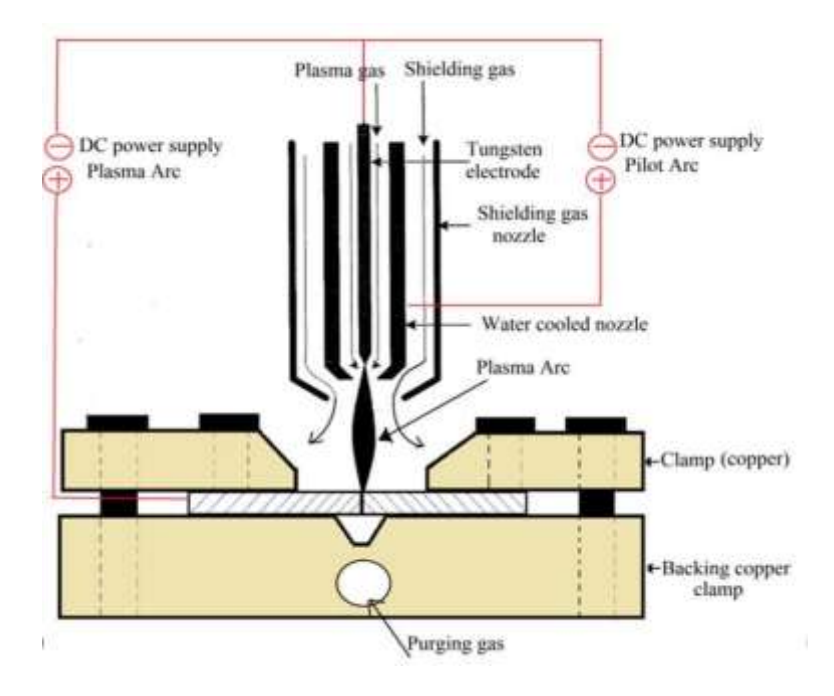


Fig. 3: Schematic diagram for experimental setup for micro plasma arc welding

Table-1: Chemical composition of Aluminium (Al-6061) (weight %)

Al	Mg	Si	Fe	Cu	Cr	Zn	Ti	Mn	Others
95.85-98.56	0.8-1.2	0.4-0.8	0-0.7	0.15-0.4	0.04-0.35	0-0.25	0-0.15	0-0.15	0-0.15

Three metallurgical samples are cut from each joint leaving the edges of defective portion of the welded length. Defective length of weld is identified visually and by conducting dye penetrant and X-ray tests and mounted using Bakelite. Sample preparation and mounting is done as per ASTM E 3-1 standard. The hardness of the weld fusion zone of the welded samples is measured using Vickers micro hardness testing machine (Make: Shimadzu hardness equipment HMV- G 20 DT) by applying a load of 0.5 Kg as per ASTM E384. Tensile

ISSN: 2582-3930

specimens are prepared as per ASTM E8M-04 guidelines (Fig. 4) using wire cut Electro Discharge Machining in the transverse direction of the weld from each welded sample.

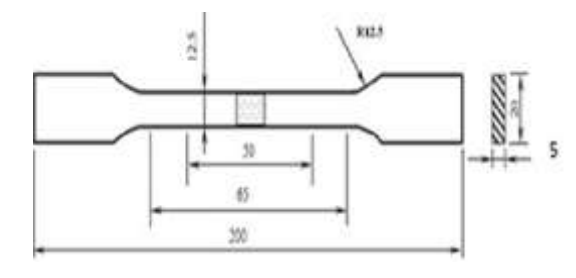


Fig. 4: Tensile specimen as per ASTM E8M-04

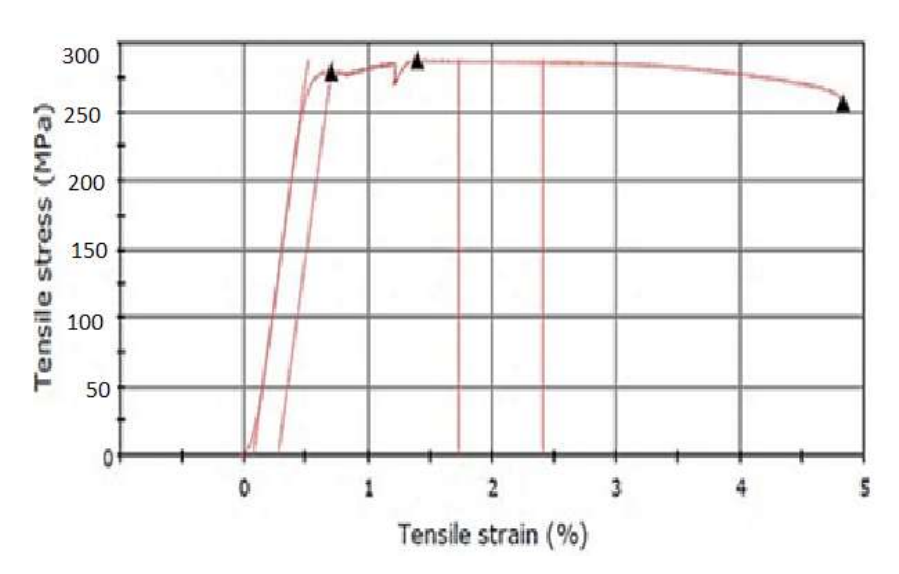


Fig. 5: Stress strain curve

3. Results and Discussion

3.1 MAIN EFFECT PLOTS FOR GRAIN SIZE, HARDNESS AND ULTIMATE TENSILE STRENGTH

Main effects of grain size, hardness and Ultimate Tensile Strength (UTS) are presented in Figs. 6, 7 and 8.

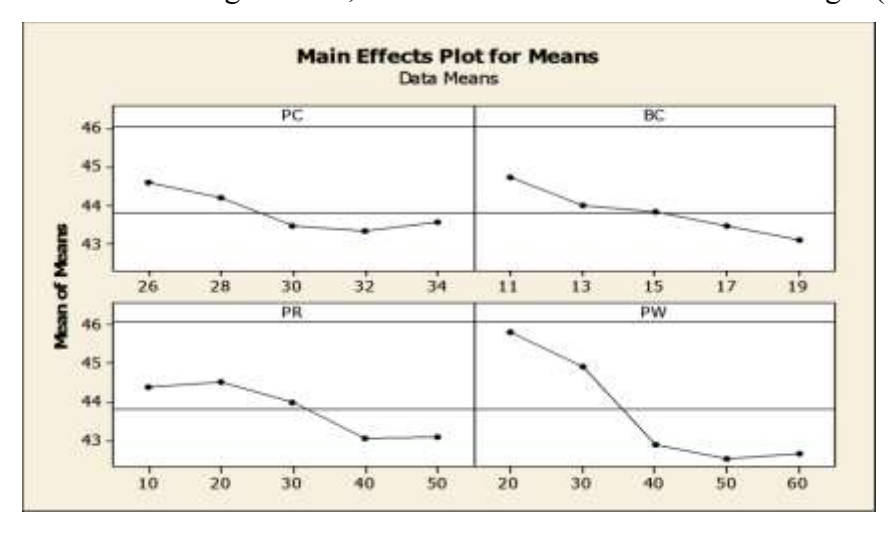


Fig. 6: Main effects of grain size

When peak current is increased from 26 Amperes to 34 Amperes, the grain size decreases because of change in cooling rate, Slower the cooling rate during solidification, the longer the time available for grain coarsening. It is well established that in welding process that cooling rate affects the grain formation. Cooling rate is usually controlled with help of purging gas during the welding process. Cooling rate can be calculated as the ratio of change in temperature to the change in time. So, to measure the cooling rate, one must record temperature and time for cooling during the welding process. In contrast, the decrease in peak current leads to the decrease in the heat input, which leads to faster cooling rate and subsequently finer grain size in fusion zone

When the pulse rate increases to 50 pulses/second, the grain size is decreased. The finer grain size of fusion zone is responsible for the increase in strength of the welded joints. At high pulse rate values, the weld molten pool is agitated violently, resulting in grain refinement in the weld region.

Pulse width of 50%, the grain size is lower. Pulse width promotes the grain growth in the weld region. As the pulse on time increases, the period from the start of

a pulse to the end of the base time also increases. When pulse width is increased, the welding heat has more time to conduct into the fusion zone, which promotes grain coarsening. The grains in fusion zone get coarser, with increasing pulse on time and the strength of these welded joints decreases.

At low welding currents the heat input will be low and time required for cooling of weldment is comparatively less with respect higher welding currents. Columnar grains are obtained at low cooling rates and fine grains are obtained at high cooling rates, which is controlled by purging gas used in welding process.

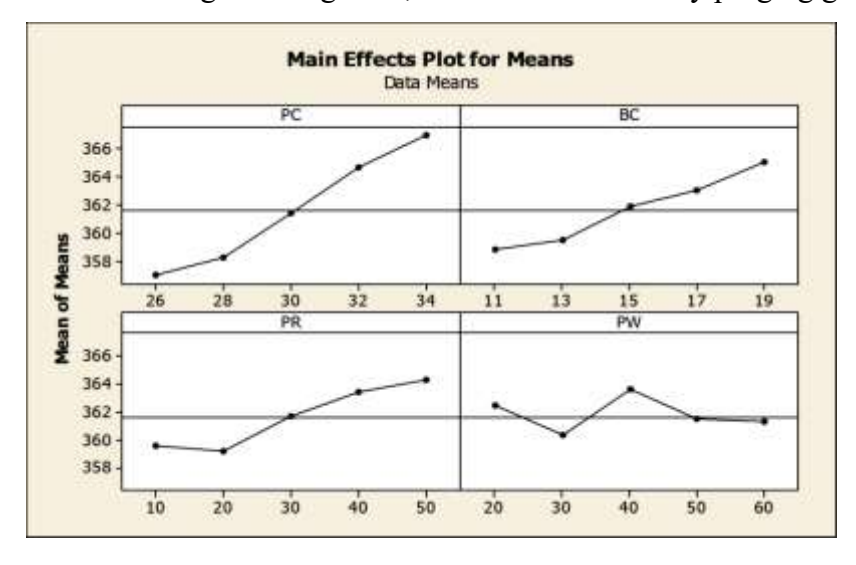


Fig. 7: Main effects of hardness

At peak current of 34 Amperes, the hardness is higher. The formation of fine equiaxed grains in fusion zone increases the hardness of the welded joints. Higher amperage and higher peak current lead to more heat and longer cooling time resulting in coarse grains, which is responsible for lower hardness. This is in line with the variation of fusion zone grain size. Hardness increases gradually with increase in base current from 26 Amperes to 34 Amperes

At a pulse rate is 20 pulses/second, the hardness is lower. When the pulse rate is increased to 50 pulses/second,

the hardness is increased. The finer grain size of fusion zone is responsible for the increase in hardness of the welded joints. At very low pulse rates, the effect of pulsing on the weld bead is less compared to that at high frequency pulsing. At high pulse rate values, the molten bead is agitated violently, resulting in grain refinement in the weld region.

At a pulse width of 30%, the hardness is lower. The pulse width promotes the grain growth in the weld region, as the pulse on time increases, the period from the start of a pulse to the end of the base time also increases. When pulse width is increased, the welding heat has more time to conduct into the fusion zone promoting grain coarsening. The grains in fusion zone get coarser, with increasing pulse on time and the hardness of these welded joints decreases.

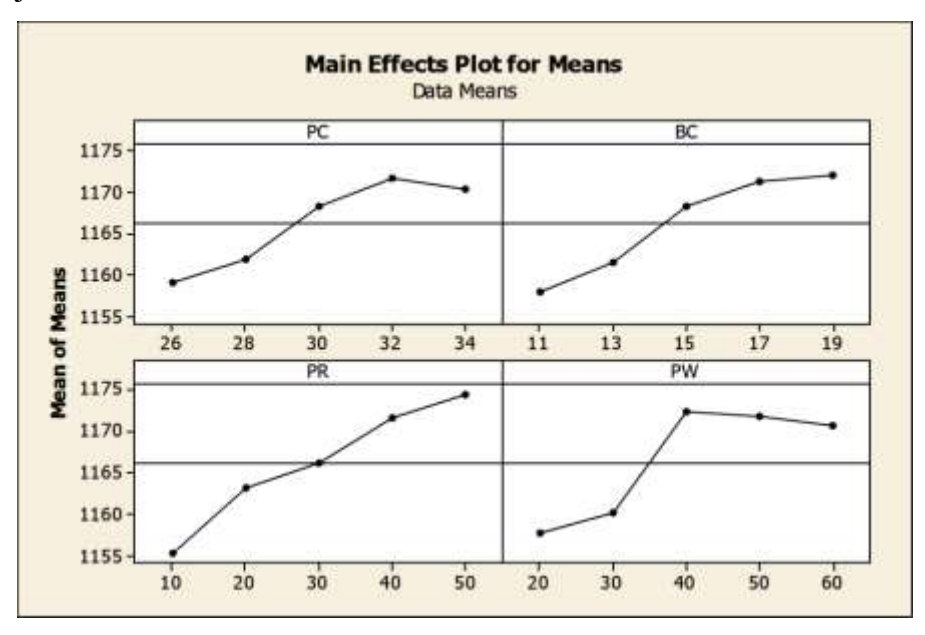


Fig. 8: Main effects of UTS

At a peak current of 32 Amperes, the ultimate tensile strength is higher. The formation of fine equiaxed grains in fusion zone increases the hardness, thereby increasing the ultimate tensile strength of the welded joints. Higher amperage and higher peak current leads to more heat and longer cooling time resulting in coarse grains, which is responsible for lower hardness and ultimate tensile strength. This is in line with the variation of fusion zone grain size. Ultimate tensile strength increases gradually with increase in base current from 11 Amperes to 19 Amperes.

At a pulse rate is 10 pulses/second, the ultimate tensile strength is lower. When the pulse rate is increased to 50 pulses/second, the ultimate tensile strength is increased. The finer grain size of fusion zone is responsible for the increase in hardness of the welded joints. At very low pulse rates, the effect of pulsing on the weld bead is less compared to that at high frequency pulsing. At high pulse rate values, the molten bead is agitated violently, resulting in grain refinement in the weld region.

At a pulse width of 20%, the hardness is lower. The pulse width promotes the grain growth in the weld region. This is because as the pulse on time increases, the

period from the start of a pulse to the end of the base time also increases. When pulse width is increased, the

welding heat has more time to conduct into the fusion zone, which promotes grain coarsening. The grains in fusion zone get coarser, with increasing pulse on time and the ultimate tensile strength of these welded joints decreases.

3.2 MATHEMATICAL MODELLING FOR GRAIN SIZE, HARDNESS AND ULTIMATE TENSILE STRENGTH

A low order polynomial is some region of the independent variables is employed to develop a relation between the response and the independent variables. If the response is well modeled by a linear function of the independent variables, then the approximating function in the first order model is

$$Y = b_0 + \alpha b_i x_i + \alpha$$

where b_0 , b_i are the coefficients of the polynomial and α represents noise.

Using MINTAB software by considering the linear model empirical models are developed.

Grain size =
$$55.06 - 0.1461 X_1 - 0.164364 X_2 - 0.0358929 X_3 - 0.0831188 X_4$$

Hardness =
$$306.772 + 1.3193 X_1 + 0.799007 X_2 + 0.138561 X_3 - 0.0210227 X_4$$

UTS =
$$1063.89 + 1.6165 X_1 + 1.80922 X_2 + 0.448043 X_3 + 0.331278 X_4$$

where X1, X2, X3, X4 represents the coded values of peak current, base current, pulse rate and pulse width.

3.3 ANALYSIS OF VARIANCE (ANOVA) FOR GRAIN SIZE, HARDNESS AND ULTIMATE TENSILE STRENGTH

The adequacy of the developed models is tested using the ANOVA. As per this technique, if the calculated value of the $F_{\rm ratio}$ of the developed model is less than the standard $F_{\rm ratio}$ (F-table value 2.355) value at a desired level of confidence of 95%, then the model is said to be adequate within the confidence limit. ANOVA test results are presented in Table-5.6 for grain size, hardness, and Ultimate Tensile Strength. From Table-2 it is understood that the developed mathematical models are found to be adequate at 95% confidence level. Coefficient of determination ' R^2 ' for the above developed models is found to be about 0.93.

Table-2: ANOVA Table for grain size, hardness and ultimate tensile strength

ANOVA TABLE FOR FUSION ZONE GRAIN SIZE									
Source	DF Seq.	SS	Adj SS	Adj MS	F	P	%C		
PC	4	5.8674	5.3742	1.3435	5.12	0.024	9		
BC	4	7.5308	4.4578	1.1144	4.25	0.039	12		
PR	4	9.9262	6.8393	1.7098	6.52	0.012	16		
PW	4	36.4371	36.4371	9.1093	34.74	0.000	58		
Error	8	2.0975	2.0975	0.2622					
Total	24	61.8590							
S = 0.512045 R-Sq = 96.61% R-Sq(adj) = 89.83%									
ANOVA TABLE FOR MICRO HARDNESS									
Source	DF Seq.	SS	Adj SS	Adj MS	F	P	%C		
PC	4	354.445	332.288	83.072	26.38	0.000	57%		
BC	4	128.324	128.408	32.102	10.19	0.003	20%		
PR	4	102.738	105.718	26.430	8.39	0.006	16%		



International Journal of Scientific Research in Engineering and Management (IJSREM)

Volume: 09 Issue: 07 | July - 2025 SJIF Rating: 8.586 **ISSN: 2582-3930**

PW	4	4.911	4.911	1.228	0.39	0.811	7%			
Error	8	25.196	25.196	3.149						
Total	24	615.614								
S = 1.77468 R-Sq = 95.91% R-Sq(adj) = 87.72%										
ANOVA TABLE FOR UTS										
Source	DF Seq.	SS	Adj SS	Adj MS	F	P	%C			
PC	4	606.40	530.73	132.68	5.09	0.025	18%			
BC	4	778.76	620.18	155.05	5.94	0.016	24%			
PR	4	1130.18	1058.51	264.63	10.14	0.003	34%			
PW	4	645.47	645.47	161.37	6.18	0.014	20%			
Error	8	208.73	208.73	26.09						
Total	24	3369.54								
S = 5.10793 R-Sq = 93.81% R-Sq(adj) = 81.42%										

where, SS = Sum of squares, MS = Mean square, DF = Degrees of freedom, F = Fishers value, %C = Contribution

3.4 Temperature fields in the x-z plane of the welding plate

Fig 9 illustrates the temperature distributions in x-z plane at different regions away from the weld centre. It is known that maximum heat is generated by the tool shoulder and the pin has very little contribution in the heat generation. The pin is mostly used for penetration to the workpiece in the dwell stage and stirring of the material during welding. Fig. 9 (a) exhibits the temperatures along the x-z surface when the tool is at 50mm along the plate length. Here the material experiences heat because of the tool shoulder as well as the pin. When moving further away from the weld centre the temperature goes on decreasing as in fig. 9 (c). Also, it can be noticed that maximum temperature is experienced at the top of the plate due to frictional heat generated between the tool shoulder and the workpiece. This heat gets conducted to the bottom of the plate because of high conductive nature of the aluminium alloy. When at 10mm away from the weld as in fig. 9 (d), the temperature rises again because at the boundary of the tool shoulder, the surface velocity is high.

Volume: 09 Issue: 07 | July - 2025 SJIF Rating: 8.586 **ISSN: 2582-3930**

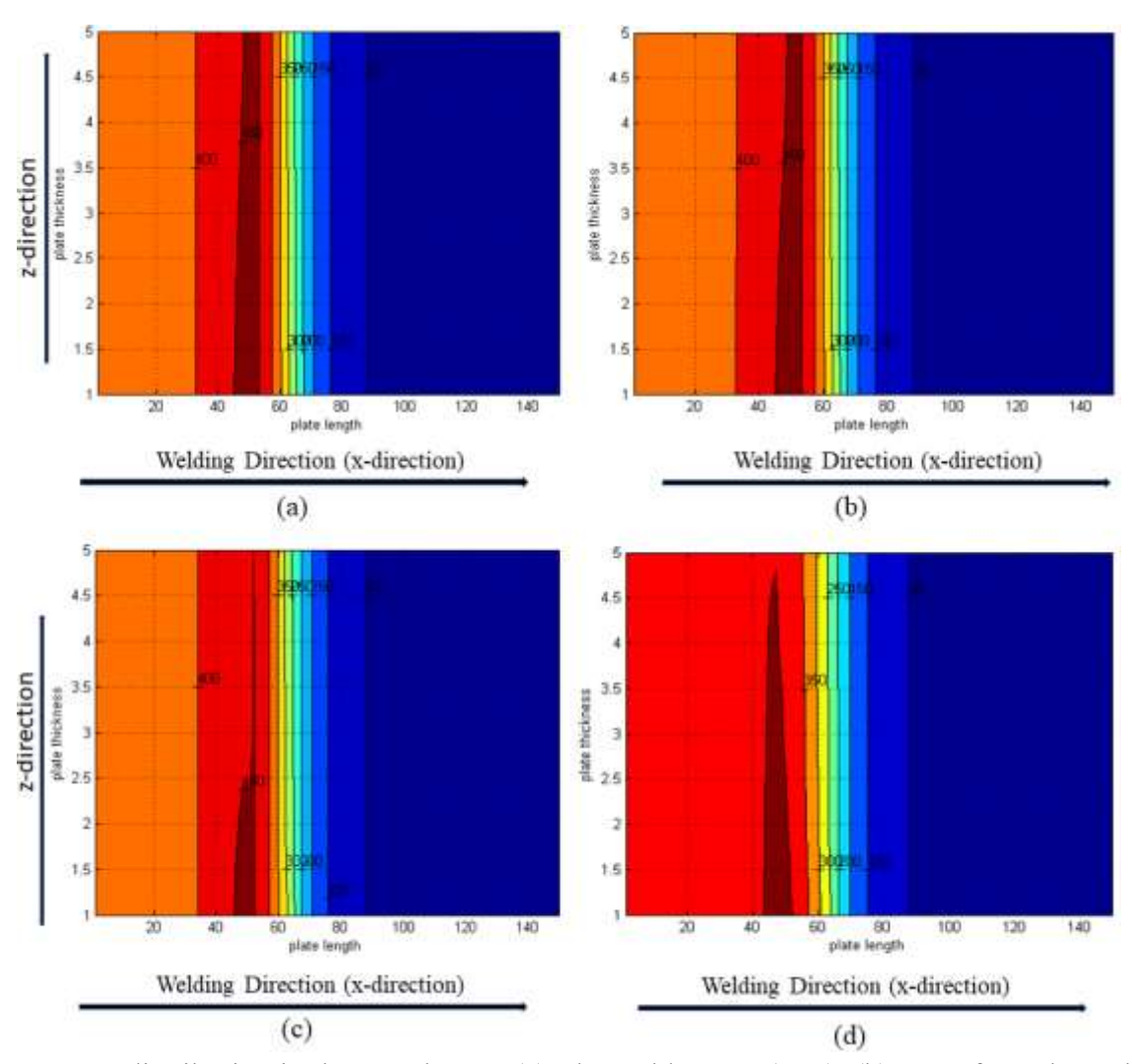


Fig. 9 Temperature distribution in the x-z plane at (a) The weld centre (y=0), (b) 3mm from the weld (c) 6mm from the weld (d) at y=10mm from the weld

4. Conclusions

- Aluminium (Al-6061) alloy is butt welded using Pulsed current Micro Plasma Arc Welding at different combinations of welding parameters as per the Taguchi Design Matrix.
- Fusion zone grain decreases with increases in peak current and base current. This is because of change in cooling rate. Slower the cooling rate during solidification, the longer the time available for grain coarsening. When the pulse rate increased, the grain size is decreased. At high pulse rate values, the weld molten pool is agitated violently, resulting in grain refinement in the weld region. When pulse width is increased, the welding heat has more time to conduct into the fusion zone, which promotes grain coarsening.
- The formation of fine equiaxed grains in fusion zone increases the hardness and ultimate tensile strength of the welded joints. Higher amperage and higher peak current lead to more heat and longer cooling time resulting in coarse grains, which is responsible for lower hardness and tensile strength. This is in line with the variation of fusion zone grain size. When the pulse rate is increased, the hardness and tensile strength are increased.
- The finer grain size of fusion zone is responsible for the increase in hardness and tensile strength of the

welded joints. At high pulse rate values, the molten bead is agitated violently, resulting in grain refinement in the weld region.

When pulse width is increased, the welding heat has more time to conduct into the fusion zone promoting grain coarsening. The grains in fusion zone get coarser, with increasing pulse on time and the hardness and tensile strength of these welded joints decreases.

References

- [1] Plasma and TIG processes Automatic welding applications, www.airliquide.com.
- [2] H.B. Cary, (1979), Modern Welding Technology, Prentice-Hill, Englewood Cliffs, New Jersey.
- [3] M. Ashraf Imam and A.C.Fraker, Titanium alloys as implant materials, Medical application of titanium and its alloy, The Material and biological Issues, ASTM STP 1272, 1996, pp. 1-16
- [4] Australian stainless steel Development Association (ASSDA), (2006), A Technical bulletin 200 series stainless steel CRMN grades, 1(10), pp. 2-3.
- [5] R.R. Boyer, "An overview on the use of titanium in the aerospace industry," Materials Science and Engineering: A, Vol. 213, No. 1-2, pp. 103-114, Aug. 1996.
- [6] G.W. Meetham, Ed., the Development of Gas Turbine Materials. Dordrecht: Springer Netherlands, 1981.
- [7] F.H.S. Froes and M.A. Imam, "Cost Affordable Developments in Titanium Technology and Applications," Key Engineering Materials, Vol. 436, May, pp. 1-11, 2010.
- [8] M.J. Donachie, Titanium: A Technical Guide, 2nd ed. ASM International, 2000.
- [9] G. Lütjering and J.C. William, Titanium. Springer-Verlag Berlin Heidelberg New York, 2003.
- [10] C. Leyens and M. Peters, Titanium and titanium alloys: Fundamentals and applications. Wiley VCH, 2003.
- [11] Dowling, Norman E., Mechanical Behavior of Materials, Prentice Hall (Upper Saddle River, NJ), 1999.
- [12] S.J. Maddox, Fatigue strength of welded structures. Abington Publishing, 1991.
- [13] Anil Kumar Nag, K.V.U. Praveen and Vakil Singh, Low cycle fatigue behavior of Ti–6Al–5Zr–05Mo–025Si alloy at room temperature, *Indian Academy of Sciences, Bull Mater Sci.*, Vol. 29, No. 3, 2006, pp. 271-275.
- [14] Nurdin Ali, M.S. Mustapa, M.I. Ghazali, T. Sujitno and M. Ridha, Fatigue Life Prediction of Commercially Pure Titanium after Nitrogen Ion Implantation, *International Journal of Automotive and Mechanical Engineering*, Vol. 7, 2013, pp. 1005-1013.
- [15] Nikolas Hrabea, Fatigue Properties of a Titanium Alloy Ti-6Al-4V Fabricated Via Electron Beam Melting EBM: Effects of Internal Defects and Residual Stress, National Institute of Standards and Technology, *International Journal of Fatigue*, Vol. 94, 2017, pp. 202-210.

- [16] M. Benedetti Cazzolli, V. Fontanari, M. Leoni, Fatigue limit of Ti6A14V alloy produced by selective laser sintering, *21*st European Conference on Fracture, ECF21, 20-24 June 2016, Catania, Italy.
- [17] Xipeng Tan, YihongKok, Yu Jun Tan, Marion Descoins, Dominique Mangelinck, ShuBengTor, Kah Fai Leong, Chee Kai Chua, Graded microstructure and mechanical properties of additive manufactured Ti–6Al–4V via electron beam melting, *Acta Materialia*, Vol. 97, 2015, pp. 1-16.
- [18] L.W. Tsay and C.Y. Tsay, The effect of microstructures on the fatigue crack growth in Ti-6AI-4V laser welds, *International Journal of Fatigue*, Vol. 19, 1997, No. 10, pp. 713-720.
- [19] Jayanthi Parthasarathya, Binil Starlya, Shivakumar Ramana, Andy Christensenb, Mechanical evaluation of porous titanium Ti6Al4V structures with electron beam melting, *Journal of the mechanical behavior of bio medical materials*, Vol. 3, 2010, pp. 249-259.
- [20] Aifeng Huang, Weixing Yao, and Fang Chen, Analysis of Fatigue Life of PMMA at Different Frequencies Based on a New Damage Mechanics Model, *Hindawi Publishing Corporation Mathematical Problems in Engineering*, Vol. 4, 2014, pp. 1-8.
- [21] Prashanth, A., Dr. K. Elangovan, Rodriguez Arthurs, Design and analysis of Ti6AL4V Titanium specimens for enhancing fatigue life performance using ultrasonic impact treatment, *International journal of Engineering Research*, Vol. 5, 2016, pp. 1129-1254.
- [22] Luca Boccarusso, Giuseppe Arleo, Antonello Astarita, Franco Bernardo, Piero De Fazio, Massimo Durante, Fabrizio Memola Capece Minutolo, Raffaele Sepe & Antonino Squillace, A new approach to study the influence of the weld bead morphology on the fatigue behavior of Ti–6Al 4V laser beam- welded butt joints, *International Journal Advanced Manufacturing Technology*, Vol. 88, 2017, pp. 75-88.
- [23] Anil Patnaik, Narendra Poondla, Udaykar Bathini, and T.S. Srivatsan, The Fatigue Behavior of Built-Up Welded Beams of Commercially Pure Titanium, *ASM International, JMEPEG*, Vol. 20, 2011, pp. 1247-1255.
- [24] Hong-Yu Qi, Hao Shi, Shao-Lin Li, Xiao-Guang Yang, Fatigue crack growth of titanium alloy joints by electron beam welding, *Rare Metals*, Vol. 5, 2014, pp. 516-521.
- [25] T.S. Balasubramanian, V. Balasubramanian and M.A. Muthumanikkam, Effect of Welding Processes on Fatigue Properties of Ti-6Al-4V Alloy Joints, *World Academy of Science, Engineering and Technology International Journal of Mechanical and Mechatronics Engineering*, Vol. 5, No. 2, 2011, pp. 427-436.